

Solution of the Cauchy problem using iterated Tikhonov regularization

A Cimetière¹, F Delvare¹, M Jaoua² and F Pons¹

¹ L3MA, Université de Poitiers & ENSMA, Laboratoire de Modélisation Mécanique et de Mathématiques Appliquées, Boulevard Pierre et Marie Curie, BP 30179, 86962 Chasseneuil Futuroscope Cedex, France

² ENIT-LAMSIN, Ecole Nationale d'Ingénieurs de Tunis, Laboratoire de Modélisation Mathématique et Numérique dans les Sciences de l'Ingénieur, BP 37, 1002 Tunis, Tunisia

E-mail: cimetiere@l3ma.univ-poitiers.fr, delvare@l3ma.univ-poitiers.fr, mohamed.jaoua@enit.rnu.tn and pons@l3ma.univ-poitiers.fr

Received 4 July 2000, in final form 6 February 2001

Abstract

We are interested in this paper in recovering lacking data on some part of a domain boundary, from the knowledge of Cauchy data on the other part. It is first proved that the desired solution is the unique fixed point of some appropriate operator, which naturally gives rise to an iterative process that is proved to be convergent. Discretization provides an additional regularization: the algorithm reads as a least square fitting of the given data, with a regularization term the effect of which fades as iterations go on. Displayed numerical results highlight its accuracy, as well as its robustness.

1. Introduction

We consider in this paper the inverse problem of recovering lacking data on some part of the boundary of a domain from Cauchy data on the other part. We shall be presenting the issue in the framework of the steady state heat equation, although the algorithm works as well in the case of elastostatics, and may be extended to various operators. Given a heat flux ψ_d on a part Γ_d of the boundary of an open set Ω , and measuring the temperature φ_d on Γ_d , it has been proved in several situations that this information is enough to recover flaws inside the body, such as inclusions or cracks, provided the given flux is properly chosen. Intending to use fast algorithms based on the reciprocity gap [2, 3, 6], one needs, however, to hold complete data (i.e. data on the whole boundary), which is not a realistic requirement in several situations where parts of this boundary are not accessible to measurements. The recovery of the lacking data from the measured ones thus appears as a mandatory first step in the reconstruction process. In a somewhat different problem, such as identification of an exchange coefficient arising in corrosion detection [7, 11, 14], recovery of the lacking data may also be a way to solve.

Provided the data (φ_d, ψ_d) we are trying to extend are compatible, which means that this pair is indeed the trace of a single harmonic function (i.e. $\varphi_d = u|_{\Gamma_d}$; $\psi_d = \partial_n u|_{\Gamma_d}$ for some

harmonic function u), such an attempt seems reasonable. Due to noise effects, compatible data are, however, not expected and, on the other hand, the Cauchy problem is well known—since Hadamard—to be severely ill posed: given any pair (φ_d, ψ_d) on Γ_d , it is possible to approximate it as closely as desired on Γ_d by the traces of a single harmonic function, the price to pay for that being a hectic behaviour of this function on the remaining part of the boundary [4, 5]. Actually, this is a result of the density of the compatible data in the space of incompatible ones, which makes it impossible to get a least squares fitting of the incompatible data by compatible ones. Regularization is thus needed to define an analogy to the Moore–Penrose pseudo-inverse operator, and not only to provide this latter with continuity [10, 16].

In this paper, we use an iterated Tikhonov regularization method [9, 13], the additional regularizing term being the distance between two successive iterated solutions. This choice makes the term fade while proceeding along with the algorithm, which eventually provides us, in the case the data to extend are compatible, with the solution of the genuine inverse problem, not with that of some problem close to it [8]. We first characterize the extended solution as the fixed point of an appropriate operator, and analyse the convergence of the algorithm starting from this point. Strong convergence is proved on the part Γ_d of the boundary, whereas only weak convergence is achieved on the remaining part of the boundary. If the reconstructed data are intended to be used in a reciprocity gap-based algorithm, such a weak convergence might be sufficient since these data are only needed for the computation of boundary integrals. However, strong convergence is also achieved provided the solution and the boundary are smooth enough.

The issue remains open for the continuous case of incompatible data, for it is not clear which ‘solution’ the algorithm should converge to. Nonetheless, discretization using a proper finite element scheme brings back the problem to the usual framework [10], yielding a convergence result dependent on the mesh size. Numerical results show accuracy and robustness.

2. The data completion problem

2.1. Notations and preliminary results

Let Ω be an open bounded set in \mathbb{R}^2 or \mathbb{R}^3 , with a smooth boundary Γ . Moreover, let us consider a partition of this boundary

$$\Gamma = \bar{\Gamma}_d \cup \bar{\Gamma}_u$$

where Γ_d and Γ_u are open parts of the boundary with positive measures.

The problem we are dealing with is to reconstruct a harmonic function u that fits some prescribed data on Γ_d . The solution we are trying to recover then belongs to the set

$$\mathcal{H}(\Omega) := \{v \in H^1(\Omega); \Delta v = 0 \text{ in } \Omega\}. \quad (1)$$

$\mathcal{H}(\Omega)$ is obviously a closed subset of $H^1(\Omega)$, which makes it a Hilbert space when equipped with the $H^1(\Omega)$ scalar product. Moreover, it is a subspace of

$$H(\Delta; \Omega) := \{v \in H^1(\Omega); \Delta v \in L^2(\Omega)\}$$

which makes it possible to define the normal derivative traces of functions belonging to this space, as elements of $H^{-\frac{1}{2}}(\Gamma)$. Therefore, the traces $(v|_\Gamma, \partial_n v|_\Gamma)$ of $\mathcal{H}(\Omega)$ functions span the space $\mathcal{H}(\Gamma)$ of *compatible data pairs*:

$$\mathcal{H}(\Gamma) := \{\phi = (\varphi, \psi) \in H^{\frac{1}{2}}(\Gamma) \times H^{-\frac{1}{2}}(\Gamma); \exists v \in \mathcal{H}(\Omega) \text{ such that } v|_\Gamma = \varphi \text{ and } \partial_n v|_\Gamma = \psi\} \quad (2)$$

and the following result holds.

Lemma 1. $\mathcal{H}(\Gamma)$ is a closed subspace of $H^{\frac{1}{2}}(\Gamma) \times H^{-\frac{1}{2}}(\Gamma)$, and it is therefore a Hilbert space when equipped with the scalar product:

$$\langle \phi, \phi' \rangle_{\Gamma} := \langle \varphi, \varphi' \rangle_{\frac{1}{2}, \Gamma} + \langle \psi, \psi' \rangle_{-\frac{1}{2}, \Gamma}. \tag{3}$$

Proof. Let (φ_k, ψ_k) be a sequence in $\mathcal{H}(\Gamma)$, convergent to $(\varphi, \psi) \in H^{\frac{1}{2}}(\Gamma) \times H^{-\frac{1}{2}}(\Gamma)$. We need to prove that $(\varphi, \psi) \in \mathcal{H}(\Gamma)$.

Let u_k and u solve in $H^1(\Omega)$ the following Dirichlet problems:

$$\begin{aligned} \Delta u_k &= 0 & \text{in } \Omega & & \Delta u &= 0 & \text{in } \Omega \\ u_k &= \varphi_k & \text{on } \Gamma & & u &= \varphi & \text{on } \Gamma. \end{aligned} \tag{4}$$

The mapping

$$\begin{aligned} H^{\frac{1}{2}}(\Gamma) &\longmapsto H^1(\Omega) \\ \varphi &\longmapsto u \end{aligned} \tag{5}$$

is continuous, yielding $\lim_{k \rightarrow 0} \|u_k - u\|_{1, \Omega} = 0$. Moreover, this convergence holds in $H(\Delta; \Omega)$ and hence $\lim_{k \rightarrow 0} \|\partial_n u_k - \partial_n u\|_{-\frac{1}{2}, \Gamma} = 0$. We derive that

$$\varphi = u|_{\Gamma} \quad \text{and} \quad \psi = \partial_n u|_{\Gamma}$$

which means $(\varphi, \psi) \in \mathcal{H}(\Gamma)$. □

Remark. According to the above result, the mapping

$$\begin{aligned} \mathcal{H}(\Omega) &\longmapsto \mathcal{H}(\Gamma) \\ u &\longmapsto (u|_{\Gamma}, \partial_n u|_{\Gamma}) \end{aligned} \tag{6}$$

is an isomorphism. There is thus no confusion in denoting by u either an element of $\mathcal{H}(\Omega)$ or the related compatible boundary pair $(u|_{\Gamma}, \partial_n u|_{\Gamma}) \in \mathcal{H}(\Gamma)$, which we shall often do for the sake of simplicity.

\mathcal{H}_d , or $\mathcal{H}(\Gamma_d)$, is the space of restrictions to Γ_d of compatible pairs. Elements of $H^{-\frac{1}{2}}(\Gamma_d)$ are restrictions to Γ_d of distributions in $H^{-\frac{1}{2}}(\Gamma)$. $H^{-\frac{1}{2}}(\Gamma_d)$ is thus the dual space of $H_{00}^{\frac{1}{2}}(\Gamma_d)$, which is the subspace of functions of $H^{\frac{1}{2}}(\Gamma_d)$ continuously extendable by zero as elements of $H^{\frac{1}{2}}(\Gamma)$ (see [12]). Given $\tau \in H^{-\frac{1}{2}}(\Gamma)$, its restriction τ_d is thus defined by

$$\langle \tau_d, \varphi_d \rangle := \langle \tau, \tilde{\varphi}_d \rangle \quad \forall \varphi_d \in H_{00}^{\frac{1}{2}}(\Gamma_d)$$

where $\tilde{\varphi}_d$ stands for the extension by zero of φ_d to the whole boundary. \mathcal{H}_u is defined in a similar way.

Let us denote by X (or by $X(\Gamma)$) the space $H^{\frac{1}{2}}(\Gamma) \times H^{-\frac{1}{2}}(\Gamma)$, and by X_d the space $H^{\frac{1}{2}}(\Gamma_d) \times H^{-\frac{1}{2}}(\Gamma_d)$. Given two elements u and v in $H(\Delta; \Omega)$, let us define

$$\langle u, v \rangle_{\Gamma} := \langle u, v \rangle_{\frac{1}{2}, \Gamma} + \langle \partial_n u, \partial_n v \rangle_{-\frac{1}{2}, \Gamma}.$$

Given $u \in H(\Delta; \Omega)$ and a pair $\phi := (\varphi, \psi) \in H^{\frac{1}{2}}(\Gamma) \times H^{-\frac{1}{2}}(\Gamma)$, let us also denote

$$\langle u - \phi, v \rangle_{\Gamma} := \langle u - \varphi, v \rangle_{\frac{1}{2}, \Gamma} + \langle \partial_n u - \psi, \partial_n v \rangle_{-\frac{1}{2}, \Gamma}.$$

The norm induced by the scalar product in Γ will be denoted by $\| \cdot \|_{\Gamma}$. The X_d scalar product and norm are defined in a similar way.

2.2. The least square harmonic lift problem

Given now data $\phi_d = (\varphi_d, \psi_d) \in X_d$, the harmonic lift problem is the following:

$$\text{Find } u \in \mathcal{H}(\Gamma) \quad \text{such that } u = \phi_d \quad \text{on } \Gamma_d. \quad (7)$$

Problem (7) has no solution *in general*, unless the data are compatible, which means $\phi_d \in \mathcal{H}_d$. In that case, the solution is unique, thanks to the Holmgren theorem, but it does not depend continuously on the data, as pointed out by Hadamard and reported, for instance, in [15]. Data coming from measurements are not expected to be compatible, and we shall thus be interested in fitting them in a least square sense, rather than exactly. However, it was noted in [4] that such an attempt has no chance of being successful: solutions can be found as close as desired to the given data on Γ_d , provided hectic behaviours on the remaining part of the boundary are accepted. Some clues about the solution behaviour on the remaining part of the boundary are therefore needed in order to turn the least square problem into a well posed one. To this end, let us define a *pattern* $\phi \in \mathcal{H}(\Gamma)$ ‘guessing’ what the desired solution should look like, and define the cost function J_c , for any $v \in X$, as follows:

$$J_c(v) := \|v - \phi_d\|_{\Gamma_d}^2 + c \|v - \phi\|_{\Gamma}^2. \quad (8)$$

The positive weight coefficient c is essential to make the least squares fitting of the prescribed data a well posed problem. Its role may also be viewed as a balancing of the confidence put on the pattern ϕ , with respect to the one granted to the data ϕ_d . The least square harmonic lift problem (LSL) we are now interested in reads as follows:

$$\text{Find } u \in \mathcal{H}(\Gamma) \quad \text{such that } J_c(u) \leq J_c(v) \quad \forall v \in \mathcal{H}(\Gamma). \quad (9)$$

Lemma 2. *The LSL problem (9) has a unique solution characterized by*

$$\langle u - \phi_d, v \rangle_{\Gamma_d} + c \langle u - \phi, v \rangle_{\Gamma} = 0 \quad \forall v \in \mathcal{H}(\Gamma). \quad (10)$$

Proof. J_c is strictly convex and continuous on $\mathcal{H}(\Gamma)$. Since $c > 0$, we also have

$$\lim_{\|v\|_{\mathcal{H}(\Gamma)} \rightarrow \infty} J_c(v) = +\infty.$$

Problem (9) has therefore a unique solution, the characterization of which follows immediately. \square

Let us now consider the data completion problem: we are given incomplete though *compatible* data, on the part Γ_d of the boundary. Let $\phi_d = (\varphi_d, \psi_d) \in \mathcal{H}_d$ be these data. Our first goal is to find the pair $\phi = (\varphi, \psi)$ in $\mathcal{H}(\Gamma)$ that extends (φ_d, ψ_d) to the whole boundary. Behind this goal, the actual one is, given a noisy hence incompatible data pair on Γ_d , to find a compatible pair (φ, ψ) on Γ that would ‘extend’ these data in an appropriate sense.

Let $\phi = (\varphi, \psi)$ be a pair in X , and u_ϕ be the solution of the LSL problem with ϕ_d as given data and ϕ as a pattern. It should not be expected that $u_\phi|_{\Gamma}$ match ϕ (in the sense that $u_\phi|_{\Gamma} = \varphi$ and $\partial_n u_\phi|_{\Gamma} = \psi$), since ϕ is not even a compatible data pair, and the LSL solution is, moreover, required to fit ϕ_d on Γ_d . However, if it does, then obviously (φ, ψ) is a compatible pair. In that case, we are going to prove that ϕ is the desired harmonic extension of ϕ_d on the whole boundary Γ , and hence u_ϕ solves the exact lift problem (7).

Let \mathcal{T} be the operator

$$\begin{aligned} \mathcal{T} : \mathcal{H}(\Gamma) &\longmapsto \mathcal{H}(\Gamma) \\ \phi &\longmapsto u_\phi \end{aligned} \quad (11)$$

where u_ϕ solves the (LSL) problem related to (ϕ_d, ϕ) .

Theorem 1. *Assuming the given data $\phi_d = (\varphi_d, \psi_d)$ are compatible, then \mathcal{T} has a unique fixed point, which is the unique extension of these data to the whole boundary.*

Proof. Let $\phi = (\varphi, \psi)$ be a fixed point of \mathcal{T} . Then

$$\|u_\phi - \phi_d\|_{\Gamma_d}^2 \leq \|v - \phi_d\|_{\Gamma_d}^2 + c \|v - \phi\|_\Gamma^2 \quad \forall v \in \mathcal{H}(\Gamma).$$

Let now u_d be the harmonic lift of the compatible data ϕ_d , which we are going to prove is exactly u_ϕ . For $\lambda \in]-1, +1[$, let us use the above inequation with the following test functions:

$$v = (1 - \lambda)u_d + \lambda u_\phi.$$

We get

$$\|u_\phi - \phi_d\|_{\Gamma_d}^2 \leq \|(1 - \lambda)u_d + \lambda u_\phi - \phi_d\|_{\Gamma_d}^2 + c \|(1 - \lambda)u_d + \lambda u_\phi - \phi\|_\Gamma^2$$

and, since u_d matches ϕ_d on Γ_d and u_ϕ matches ϕ on Γ ,

$$\|u_\phi - \phi_d\|_{\Gamma_d}^2 \leq \lambda^2 \|u_\phi - \phi_d\|_{\Gamma_d}^2 + c(1 - \lambda)^2 \|u_d - \phi\|_\Gamma^2$$

which yields

$$\|u_\phi - u_d\|_{\Gamma_d}^2 \leq c \frac{1 - \lambda}{1 + \lambda} \|u_d - u_\phi\|_\Gamma^2.$$

By making $\lambda \rightarrow 1$, it comes out that $u_\phi = u_d$ on Γ_d , and since both of them are elements of $\mathcal{H}(\Gamma)$, this yields $u_\phi \equiv u_d$. ϕ is hence the harmonic extension of ϕ_d , which is unique. \square

Remark. It should be pointed out that this fixed point does not depend on c .

3. The fixed point process

Trying to recover the fixed point of \mathcal{T} , it is now natural to propose the following fixed point process, which turns out to be the iterated Tikhonov algorithm:

- (1) *Initialization.* Choose any pattern $u^0 \in \mathcal{H}(\Gamma)$ (actually, 0 can do)
- (2) *Iteration.* Given $u^k \in \mathcal{H}(\Gamma)$, solve the LSL problem related to (ϕ_d, u^k) in order to get $u^{k+1} = \mathcal{T}(u^k) \in \mathcal{H}(\Gamma)$, characterized by

$$\langle u^{k+1} - \phi_d, v \rangle_{\Gamma_d} + c \langle u^{k+1} - u^k, v \rangle_\Gamma = 0 \quad \forall v \in \mathcal{H}(\Gamma). \quad (12)$$

The problem we are dealing with, however, does not match the general theory reported in [10]. Defining the restriction operator

$$K : \begin{array}{l} \mathcal{H}(\Gamma) \quad \longmapsto \quad F \\ (u, \partial_n u) \quad \longmapsto \quad (u|_{\Gamma_d}, \partial_n u|_{\Gamma_d}) \end{array} \quad (13)$$

we can either choose $F := \mathcal{H}(\Gamma_d)$ or $F = X_d$. The first choice is not relevant, for F is not a Hilbert space when equipped with the $\mathcal{H}(\Gamma_d)$ scalar product, which makes K bounded, its closure being X_d . In the second case, the range of K is $\mathcal{H}(\Gamma_d)$, which is dense in F . There is hence no way to fit the prescribed data in a usual least squares sense, unless the regularizing term is added to the functional. This is the reason why the convergence results obtained here are weaker than the general theory ones [10]. Further, these results do not address noisy (i.e. incompatible) data, for there is no ‘solution’ for the algorithm to converge to in that case. However, discretization brings an additional regularization, by drawing back the problem to the general framework, as will be seen in section 4. The following lemma is the first step in the convergence proof in the continuous case.

Lemma 3. *The sequence $(u^k)_{k \geq 1}$ produced by the fixed point algorithm verifies for all $n \in \mathbb{N}$:*

$$\|u^{n+1} - u_d\|_{\Gamma}^2 + \sum_{k=0}^n \|u^{k+1} - u^k\|_{\Gamma}^2 + \frac{2}{c} \sum_{k=0}^n \|u^{k+1} - u_d\|_{\Gamma_d}^2 = \|u^0 - u_d\|_{\Gamma}^2. \tag{14}$$

Proof.

$$\begin{aligned} \|u^{k+1} - u_d\|_{\Gamma}^2 &= \langle (u^{k+1} - u^k) + (u^k - u_d), (u^{k+1} - u^k) + (u^k - u_d) \rangle_{\Gamma} \\ &= \|u^k - u_d\|_{\Gamma}^2 + \|u^{k+1} - u^k\|_{\Gamma}^2 + 2\langle u^k - u_d, u^{k+1} - u^k \rangle_{\Gamma} \\ &= \|u^k - u_d\|_{\Gamma}^2 - \|u^{k+1} - u^k\|_{\Gamma}^2 + 2\langle u^{k+1} - u_d, u^{k+1} - u^k \rangle_{\Gamma}. \end{aligned} \tag{15}$$

Using the characterization (12) of u^{k+1} with $v = u^{k+1} - u_d$ as a test function, we get

$$\langle u^{k+1} - u_d, u^{k+1} - u^k \rangle_{\Gamma} = -\frac{1}{c} \|u^{k+1} - u_d\|_{\Gamma_d}^2.$$

Plotting this in (15), we obtain

$$\|u^{k+1} - u_d\|_{\Gamma}^2 + \|u^{k+1} - u^k\|_{\Gamma}^2 + \frac{2}{c} \|u^{k+1} - u_d\|_{\Gamma_d}^2 = \|u^k - u_d\|_{\Gamma}^2.$$

Adding these equalities for $0 \leq k \leq n$ then yields (14). □

Theorem 2 (Convergence of the sequence). *Let $u_d = (\varphi_d, \psi_d)$ be a given pair of compatible data on Γ_d . Therefore, the sequence $(u^k)_{k \geq 1}$ computed by the fixed point algorithm strongly converges to u_d on Γ_d , and it weakly converges on the whole boundary:*

$$\lim_{k \rightarrow \infty} \|u^k - u_d\|_{\Gamma_d} = 0.$$

Proof. From (14), we derive that

$$\sum_{k=0}^{\infty} \|u^{k+1} - u_d\|_{\Gamma_d}^2 < \infty$$

which immediately yields the strong convergence result $\lim_{k \rightarrow \infty} \|u^{k+1} - u_d\|_{\Gamma_d} = 0$.

To prove the weak convergence of the sequence on the whole boundary, let us take the following steps.

(1) Weak convergence in $\mathcal{H}(\Gamma)$ of a subsequence u^μ to u_d .

From (14), we know that $\|u^k - u_d\|_{\Gamma}$ is a bounded sequence. The sequence $(u^k)_{k \geq 1}$ is therefore a bounded sequence of $\mathcal{H}(\Gamma)$, which has been proved in lemma 1 to be a Hilbert thus reflexive space. There therefore exists a subsequence of u^k , that we shall denote by u^μ , which weakly converges in $\mathcal{H}(\Gamma)$. Let u be its limit.

Writing down the characterization equation for u^μ , with $u - u_d$ as a test function, we get

$$\langle u^\mu - u_d, u - u_d \rangle_{\Gamma_d} + c \langle u^\mu - u^{\mu-1}, u - u_d \rangle_{\Gamma} = 0.$$

Making $\mu \rightarrow \infty$ hence yields

$$\|u - u_d\|_{\Gamma_d}^2 = 0$$

from which we derive, since both functions are harmonic, that $u \equiv u_d$ on the whole boundary Γ .

(2) Weak convergence of the whole sequence. Assuming it does not hold, we derive the existence of $v \in \mathcal{H}(\Gamma)$ and $\varepsilon > 0$ such that

$$\forall N \in \mathbb{N}, \quad \exists n = n(N) > N \text{ such that } |\langle u^n - u_d, v \rangle_{\Gamma}| \geq \varepsilon.$$

This gives rise to a subsequence u^v such that

$$\forall v \in \mathbb{N}, \quad |\langle u^v - u_d, v \rangle_{\Gamma}| \geq \varepsilon. \tag{16}$$

On the other hand, u^v is bounded in $\mathcal{H}(\Gamma)$ since u^k is. It is thus possible to find out a subsequence of it which weakly converges on Γ , and since $\lim_{v \rightarrow \infty} \|u^v - u_d\|_{\Gamma_d} = 0$, its limit is necessarily u_d , which contradicts (16). □

Corollary 1 (Strong convergence on the whole boundary). *The first part of u^k (i.e. the function, not the normal derivative) coming out from the fixed point algorithm strongly converges to the first part of u_d in $L^q(\Gamma)$ for*

- $1 \leq q < \infty$ in the 2D case
- $1 \leq q < 4$ in the 3D case.

Proof. The sequence $u^k|_\Gamma$ is bounded in $H^{\frac{1}{2}}(\Gamma)$. This space is compactly embedded in $L^q(\Gamma) \forall q; 1 \leq q < \infty$ in the 2D case, and $\forall q; 1 \leq q < 4$ in the 3D case [1]. Let q be such a real number. A convergent subsequence of u^k can therefore be found in $L^q(\Gamma)$, and its limit can obviously be nothing but u_d . As for theorem 2, the whole sequence converges in $L^q(\Gamma)$. \square

Remark. Provided that the desired solution holds some extra regularity, say $u \in H^2(\Omega)$, then the whole study can be carried out in the space $H^{\frac{3}{2}}(\Gamma) \times H^{\frac{1}{2}}(\Gamma)$ instead of $H^{\frac{1}{2}}(\Gamma) \times H^{-\frac{1}{2}}(\Gamma)$. Of course, the cost function needs to be modified accordingly. Strong convergence to u_d is then derived in $H^{\frac{3}{2}}(\Gamma_d) \times H^{\frac{1}{2}}(\Gamma_d)$, as well as weak convergence in $H^{\frac{3}{2}}(\Gamma) \times H^{\frac{1}{2}}(\Gamma)$.

The key result is that this space is indeed a Hilbert one, when equipped with the appropriate scalar product:

$$\langle \phi, \phi' \rangle_\Gamma := \langle \varphi, \varphi' \rangle_{\frac{3}{2}, \Gamma} + \langle \psi, \psi' \rangle_{\frac{1}{2}, \Gamma}.$$

The estimates come out exactly the same way as described above. What is gained is the strong convergence on Γ of the normal derivatives $\partial_n u^k$ in addition to the convergence of u^k . According to the Rellich–Kondrachov and Sobolev embeddings [1], the spaces where such convergences occur are $C^{0,\beta}(\Gamma) \times L^q(\Gamma)$ with

- $\beta < 1$ and $q < \infty$ in the 2D case
- $\beta < \frac{1}{2}$ and $q < 4$ in the 3D case.

4. Numerical implementation and results

4.1. The discrete problem

The first issue in this section is to discretize the set $\mathcal{H}(\Gamma)$ the minimization problem is living in. Our main concern has been to make use of any ordinary finite element code, not to work out a peculiar one. As a matter of fact, computations have been run using *Castem 2000* and piecewise linear finite elements, which means a piecewise constant approximation for the normal derivatives. Let u be an harmonic function in $H^1(\Omega)$: we have

$$u \in \mathcal{H}(\Omega) \iff \int_\Omega \nabla u \nabla v = \int_\Gamma \frac{\partial u}{\partial n} v \quad \forall v \in H^1(\Omega). \tag{17}$$

It emerges that $\mathcal{H}(\Gamma)$ may thus be characterized as follows:

$$\mathcal{H}(\Gamma) = \left\{ (\varphi, \varphi') \in H^{\frac{1}{2}}(\Gamma) \times H^{-\frac{1}{2}}(\Gamma); \exists u \in H^1(\Omega); u|_\Gamma = \varphi \right. \\ \left. \text{and } \int_\Omega \nabla u \nabla v = \int_\Gamma \varphi' v \quad \forall v \in H^1(\Omega) \right\}. \tag{18}$$

Let us now discretize the domain Ω , h being the discretization parameter standing for the element size, leading to n nodes and n' elements on the boundary, and m nodes inside the domain. Let V_h be the space of piecewise linear functions with respect to this mesh, and let us define $V_h(\Gamma)$ and $W_h(\Gamma)$ as the spaces of piecewise linear and piecewise constant functions

on the boundary. Traces of functions belonging to $V_h(\Omega)$ span the space $V_h(\Gamma)$, whereas their normal derivatives belong to the space $W_h(\Gamma)$ of piecewise constant functions, which are in addition circulation free. It is thus natural to define

$$\mathcal{H}_h(\Gamma) = \left\{ (\varphi_h, \varphi'_h) \in V_h(\Gamma) \times W_h(\Gamma); \exists u_h \in V_h(\Omega); u_h|_\Gamma = \varphi_h \right. \\ \left. \text{and } \int_\Omega \nabla u_h \nabla v_h = \int_\Gamma \varphi'_h v_h \forall v_h \in V_h(\Omega) \right\}. \quad (19)$$

Actually, φ'_h is the normal derivative of u_h in a weak sense, not exactly.

Let us now depict the effective computational scheme implemented. Defining to this end U and U' as the n and n' vectors standing for the values of u_h and $\partial_n u_h$ on the boundary, and U^* the m -vector of internal nodal values of u_h , the discrete compatibility as set in (19) may also read as follows:

$$\begin{pmatrix} A_{11} & A_{21}^T & 0 \\ A_{21} & A_{22} & -B \end{pmatrix} \begin{pmatrix} U^* \\ U \\ U' \end{pmatrix} = \begin{pmatrix} 0 \\ 0 \\ 0 \end{pmatrix}. \quad (20)$$

Being the $m \times m$ stiffness matrix corresponding to the homogeneous Dirichlet problem, A_{11} is invertible, which allows us to perform a condensation by expressing the internal unknowns U^* in terms of the boundary ones U and U' . Equation (20) then reduces to

$$(A_{22} - A_{21} A_{11}^{-1} A_{21}^T) U - B U' = 0 \quad (21)$$

the matrix form of which is the following:

$$[(A_{22} - A_{21} A_{11}^{-1} A_{21}^T); -B] \begin{bmatrix} U \\ U' \end{bmatrix} = 0_{\mathbb{R}^n}. \quad (22)$$

The relationship (22) is actually the matrix form for the discrete compatibility as defined in [8]. Denoting by \mathcal{E}_h the linear operator mapping $\mathbb{R}^n \times \mathbb{R}^{n'}$ onto \mathbb{R}^n in (22), the approximation space $\mathcal{H}_h(\Gamma)$ is

$$\mathcal{H}_h(\Gamma) = \{(U, U') \in \mathbb{R}^n \times \mathbb{R}^{n'}; \mathcal{E}_h(U, U') = 0\}. \quad (23)$$

Given now $c > 0$ and $(U_k, U'_k) \in \mathcal{H}_h(\Gamma)$, iteration $(k+1)$ of the discretized fixed point algorithm reads as follows:

$$\text{Find } (U_{k+1}, U'_{k+1}) \in \mathcal{H}_h(\Gamma) \quad \text{such that :} \\ J_k(U_{k+1}, U'_{k+1}) \leq J_k(V, V') \quad \forall (V, V') \in \mathcal{H}_h(\Gamma) \quad (24)$$

where J_k is the discretized least square function. It should be pointed out that a $L^2 \times L^2$ norm has been used in the discrete cost function, instead of the $H^{\frac{1}{2}} \times H^{-\frac{1}{2}}$ one. Apart from reasons of simplicity, and the fact that all finite-dimensional norms are eventually equivalent³, the reason why such a choice has been adopted is that numerical trials using a $H^1 \times L^2$ norm have shown no improvement in the outcome.

Problem (24) is a minimization problem in $\mathbb{R}^n \times \mathbb{R}^{n'}$ under the n equality constraints expressed by (21), the solution of which thus verifies

$$\nabla J_k(U_{k+1}, U'_{k+1}) = \Lambda_{k+1}^T \nabla \mathcal{E}_h(U_{k+1}, U'_{k+1}) \\ \mathcal{E}_h(U_{k+1}, U'_{k+1}) = 0 \quad (25)$$

where Λ_{k+1} is the n -vector of Lagrange multipliers resulting from the equality constraints.

³ Choosing a $L^2 \times L^2$ norm involves magnifying the part of the normal derivatives with respect to the function's one in the least square function, the amplification factor being $1/h$. This is equivalent to dropping, in the least square function, the contribution of the tangential derivatives, which are calculated from the function values by numerical derivation, hence holding less accuracy yet providing no additional information.

Each iteration in the fixed point algorithm needs the solution of a $2n + n'$ linear system, the matrix of which needs to be computed only once, or more precisely only each time the coefficient c is modified, if ever. This is the reason why a direct algorithm (the Crout factorization) has been preferred to iterative methods.

4.2. Convergence of the discrete algorithm

The convergence analysis cannot be carried out in a similar way to the continuous case, since there is no discrete analogous to Holmgren's theorem to rely on. Let μ be the dimension of $\mathcal{H}_h(\Gamma)$, and ν_d the number of prescribed data. Denoting by n_d the number of nodes carried by Γ_d , we have for the above-described finite element approximation scheme in the 2D case $\nu_d = 2n_d - 1$.

Solving the 'discrete Cauchy problem' amounts to picking out in $\mathcal{H}_h(\Gamma)$ a function that exactly fits the ν_d given data. Such an attempt is obviously hopeless if $\nu_d > \mu$, in which case a least square fitting of these data would however make sense since $\langle \cdot, \cdot \rangle_{\Gamma_d}$ is a scalar product on $\mathcal{H}_h(\Gamma)$. In the opposite case $\nu_d \leq \mu$, there may be infinitely many solutions, defined up to an element from the kernel of the 'trace on Γ_d operator'. Let \mathcal{Z}_h be that kernel:

$$\mathcal{Z}_h(\Gamma) = \{z_h \in \mathcal{H}_h(\Gamma) ; z_h|_{\Gamma_d} = 0\}. \quad (26)$$

Let us denote by $\mathcal{Y}_h(\Gamma)$ its orthogonal subspace in $\mathcal{H}_h(\Gamma)$,

$$\mathcal{Y}_h(\Gamma) := \mathcal{Z}_h^\perp = \{y_h \in \mathcal{H}_h(\Gamma) ; \langle y_h, z_h \rangle_\Gamma = 0 \forall z_h \in \mathcal{Z}_h\}. \quad (27)$$

Given now any data $u_d \in H^{\frac{1}{2}}(\Gamma_d) \times H^{-\frac{1}{2}}(\Gamma_d)$, the discrete Cauchy problem is the following:

$$\text{Find } u_h^d \in \mathcal{Y}_h(\Gamma) \quad \text{such that :} \quad \langle u_h^d - \pi_h u_d, y_h \rangle_{\Gamma_d} = 0 \quad \forall y_h \in \mathcal{Y}_h(\Gamma) \quad (28)$$

where π_h is the interpolation operator from X_d onto X_d^h . Problem (28) is a well posed one, addressing both situations described above. In the first one, \mathcal{Y}_h is the whole space \mathcal{H}_h , and the solution of problem (28) is hence nothing but the least square fit of the prescribed data with respect to the norm $\| \cdot \|_{\Gamma_d}$. In the second, u_h^d also represents a least square fit, the closest one to zero among all the possible fits. Given the restriction operator τ_h ,

$$\begin{aligned} \tau_h : \mathcal{H}_h(\Gamma) &\longmapsto X_h(\Gamma_d) \\ v_h &\longmapsto v_h|_{\Gamma_d} \end{aligned} \quad (29)$$

its range is $\mathcal{H}_h(\Gamma_d)$ whereas its kernel is \mathcal{Z}_h . We are brought back to the general framework as explained in [10], u_h^d being thus nothing but the image by the Moore–Penrose pseudo-inverse operator τ_h^\dagger of the prescribed data $\pi_h u_d$:

$$u_h^d = \tau_h^\dagger(\pi_h u_d).$$

This provides the following convergence result.

Proposition 1. *Initializing with zero the algorithm (24), the outcoming sequence $(u_h^k)_{k \geq 0}$ holds the following properties:*

- (i) $u_h^k \in \mathcal{Y}_h(\Gamma) \quad \forall k \geq 0$.
- (ii) *The sequence converges to the unique solution of the discrete Cauchy problem (28).*
- (iii) *Given a mesh, and a value of the positive parameter c , there exists a positive constant α_h depending on the mesh and the partition of the boundary such that*

$$\|u_h^k - u_h^d\|_\Gamma \leq \left(\frac{c}{c + \alpha_h} \right)^k \|u_h^d\|_\Gamma. \quad (30)$$

Proof. Although the result is a straightforward consequence of the formulation of the discrete problem in the general framework [10], displaying its proof is useful to find out what the constant α_h is. u_h^{k+1} solves the minimization problem in \mathcal{H}_h , and is characterized by

$$\langle u_h^{k+1} - \pi_h u_d, v_h \rangle_{\Gamma_d} + c \langle u_h^{k+1} - u_h^k, v_h \rangle_{\Gamma} = 0 \quad \forall v_h \in \mathcal{H}_h.$$

Let $u_h^k := z_h^k + y_h^k$, with $z_h^k \in \mathcal{Z}_h(\Gamma)$ and $y_h^k \in \mathcal{Y}_h(\Gamma)$. From the above characterization, we derive

$$0 + c \langle z_h^{k+1} - z_h^k, z_h \rangle_{\Gamma} = 0 \quad \forall z_h \in \mathcal{Z}_h \quad (31)$$

and also

$$\langle y_h^{k+1} - \pi_h u_d, y_h \rangle_{\Gamma_d} + c \langle y_h^{k+1} - y_h^k, y_h \rangle_{\Gamma} = 0 \quad \forall y_h \in \mathcal{Y}_h. \quad (32)$$

From equation (31), we derive that $z_h^k = 0 \forall k \geq 1$, since $z_h^0 = 0$, and thus that $u_h^k = y_h^k \forall k \geq 1$. As for equation (32), the first part of its left-hand side can be rewritten, using the solution u_h^d of the discrete Cauchy problem (28), and we get

$$\langle u_h^{k+1} - u_h^d, y_h \rangle_{\Gamma_d} + c \langle u_h^{k+1} - u_h^k, y_h \rangle_{\Gamma} = 0 \quad \forall y_h \in \mathcal{Y}_h. \quad (33)$$

Choosing now $y_h = u_h^{k+1} - u_h^d$ in equation (33), we get

$$\|u_h^{k+1} - u_h^d\|_{\Gamma_d}^2 + c \langle u_h^{k+1} - u_h^k, u_h^{k+1} - u_h^d \rangle_{\Gamma} = 0$$

and further, by setting $u_h^{k+1} - u_h^k = (u_h^{k+1} - u_h^d) - (u_h^k - u_h^d)$:

$$\|u_h^{k+1} - u_h^d\|_{\Gamma_d}^2 + c \|u_h^{k+1} - u_h^d\|_{\Gamma}^2 \leq c \|u_h^{k+1} - u_h^d\|_{\Gamma} \|u_h^k - u_h^d\|_{\Gamma}.$$

On \mathcal{Y}_h , $\|\cdot\|_{\Gamma_d}$ defines a norm, hence equivalent to $\|\cdot\|_{\Gamma}$, and there exists some positive constant α_h such that

$$(\alpha_h + c) \|u_h^{k+1} - u_h^d\|_{\Gamma} \leq c \|u_h^k - u_h^d\|_{\Gamma}$$

which ends the proof. \square

Remarks.

- (1) Initializing the algorithm with any first guess other than zero, i.e. with $u_h^0 := y_h^0 + z_h^0$, then convergence will be achieved to $z_h^0 + u_h^d$ instead of u_h^d . Actually, the iterations only operate on the \mathcal{Y}_h component, leaving unchanged the \mathcal{Z}_h one.
- (2) Given a mesh size h , estimate (30) suggests that the smaller is c , the faster the convergence. The value $c = 0$ must, however, be avoided, for τ_h^{\dagger} is not continuous in that case.
- (3) Estimate (30) provides no clue to the behaviour of the algorithm with respect to h . For a given c , the convergence result is actually lost when $h \rightarrow 0$, since $\lim_{h \rightarrow 0} \alpha_h = 0$.

4.3. Numerical results

The numerical study of the fixed point algorithm features have been outlined in a 2D situation, the domain Ω being the disc with radius $\frac{1}{2}$ centred at $(\frac{1}{2}, \frac{1}{2})$, and the function u to be approximated being the following:

$$u(x, y) = \cos x \cosh y + \sin x \sinh y.$$

First of all, displayed in figure 1 are the reconstructed solutions using a fine regular mesh of 360 nodes on the boundary, half of which carries prescribed data. Two values of coefficient c have been considered: 10^{-5} and 10^{-8} .

Further 2D cases, as well as a 3D one, were run afterwards, in order to emphasize the algorithm's possibilities, and its limitations as well.

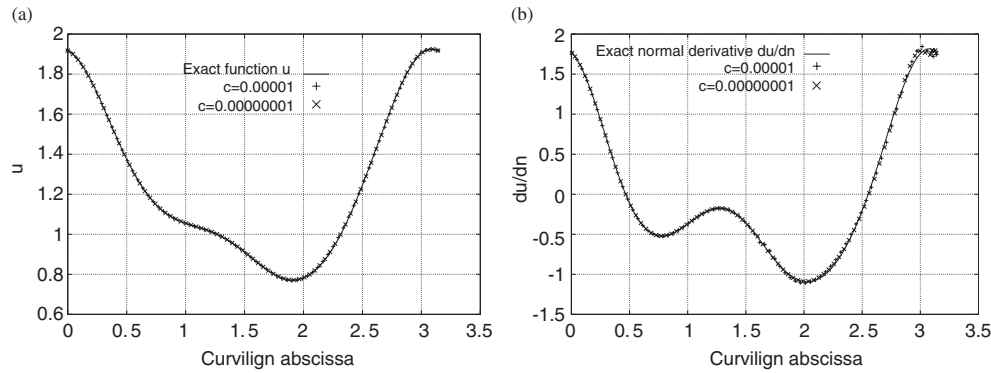


Figure 1. Reconstruction of the function (a) and its normal derivative (b).

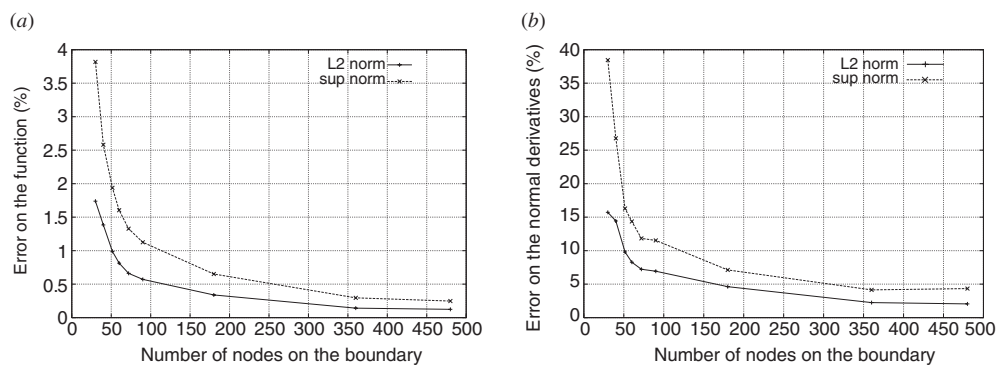


Figure 2. Errors on the function (a) and its normal derivative (b) with respect to the mesh.

4.3.1. *Behaviour with respect to the mesh.* Figure 2 displays the L^2 and L^∞ errors on the boundary, regarding both u and $\partial_n u$, with respect to the number N of nodes on the boundary. Given data have been prescribed on half of the boundary.

Fifty nodes on the boundary are enough to recover u with less than a 1% L^2 error, whereas the error on the normal derivative remains at a somewhat high (10%) level. Reducing this error to below a 5% level requires raising the mesh up to 200 nodes on the boundary. Yet, the computational time remains reasonable.

4.3.2. *Sensitivity to the c parameter.* Recall that this parameter has been introduced in order to balance the confidence put on the pattern, which is basically the reconstructed part of the solution, with respect to the one put on the prescribed data.

From a theoretical point of view, the algorithm is convergent whatever the value of c is. As noted above, estimate (30) suggests that the convergence rate improves when c decreases to zero, which is confirmed by trials reported in figure 3(b), whereas figure 3(a) shows the insensitivity of the error with respect to it.

It thus seems reasonable to choose the smallest possible value for c . From a numerical point of view, however, it has been noticed that c needs to be updated while proceeding with iterations. The reason for this is that the regularization part in the cost function, which is the distance between two successive iterates, decreases faster than the distance to the prescribed data, becoming neglectable with respect to it. Since this regularization part is ensuring well

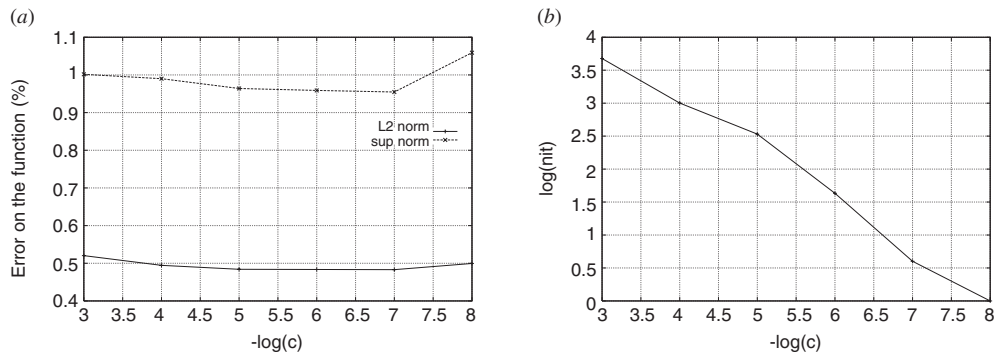


Figure 3. Errors on the function (a) and number of iterations (b) with respect to c .

posedness to the problem solved, it needs to be prevented from collapsing, which is achieved by enhancing c .

4.3.3. Sensitivity to the ratio of given data. Although the theory has nothing to do with it, it is important to study the effect of the ratio of prescribed data, with respect to the unknown ones, on the algorithm outcome. This ratio can be measured by the following single parameter ρ :

$$\rho := \frac{\text{meas}(\Gamma_d)}{\text{meas}(\Gamma)}.$$

It is not surprising that figure 4 shows improvement of both the function and normal derivative recovery when increasing this ratio.

The above ratio ρ is the objective one. From a numerical point of view, however, another relevant ratio to consider is the following:

$$\rho_h := \frac{n_d}{n}$$

where n_d is the number of nodes on the part Γ_d of the boundary, and n the total number of nodes. In the case of uniform meshes, both ratios are, of course, equivalent. An interesting issue to investigate is how sensitive to the ratio ρ_h the recovery is, for a given value of ρ , and a given total number N of nodes on the boundary, meaning a given computational cost. Numerical trials that the plots in figures 5(a) and (b) are made from were run with 360 nodes on the boundary, and $\rho = 1/6$. What can be deduced from these trials is that significant improvements in the recovery may be gained by mere redistribution of the nodes on the boundary, increasing the number of nodes on Γ_d , and hence the number of given data, and decreasing accordingly the number of those on Γ_u .

As for plots (c) and (d) in figure 5, they both display runs with $\rho = 1/4$ and $n_d = 18$, the first one with a coarse mesh using 36 nodes on the whole boundary, and the second with a fine one using 360 nodes. As expected, the accuracy is not improved by mere refinement of the mesh on Γ_u if no additional data is provided on Γ_d . This means that the reconstruction accuracy depends only on the amount of given data. What is highlighted, on the other hand, is the remarkable robustness of the algorithm, since convergence is achieved even with a very low number of prescribed data.

4.3.4. Non-smooth data. The recovery of non-smooth functions is an important issue to investigate. In the case of smooth boundaries, we mean by ‘non-smooth’ functions those

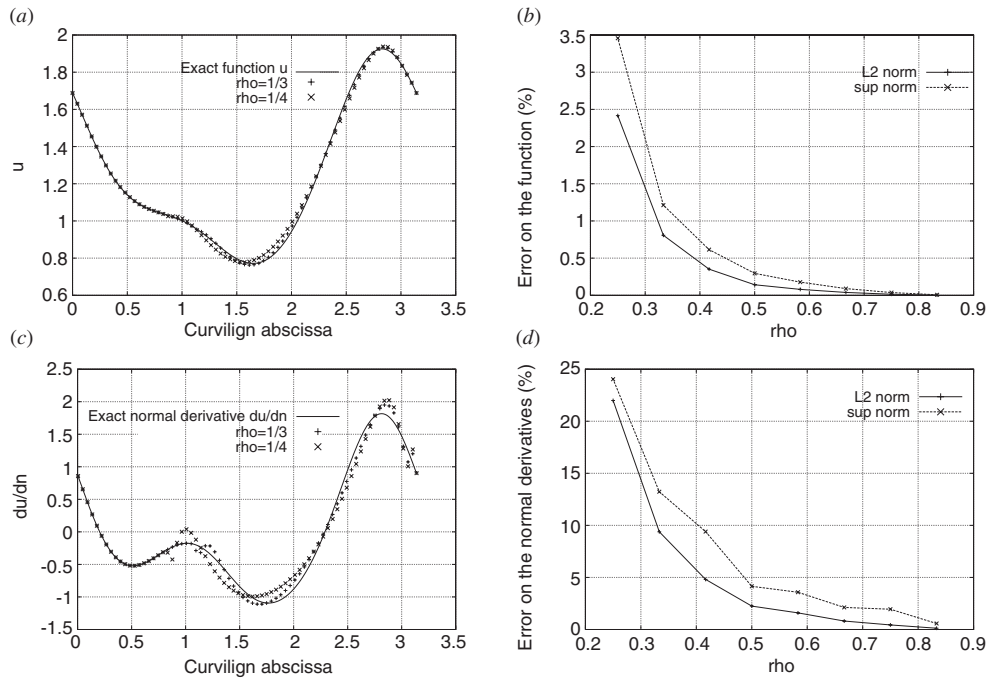


Figure 4. Reconstructed solutions (a), (c) and errors (b), (d) with respect to the ratio of given data (uniform mesh).

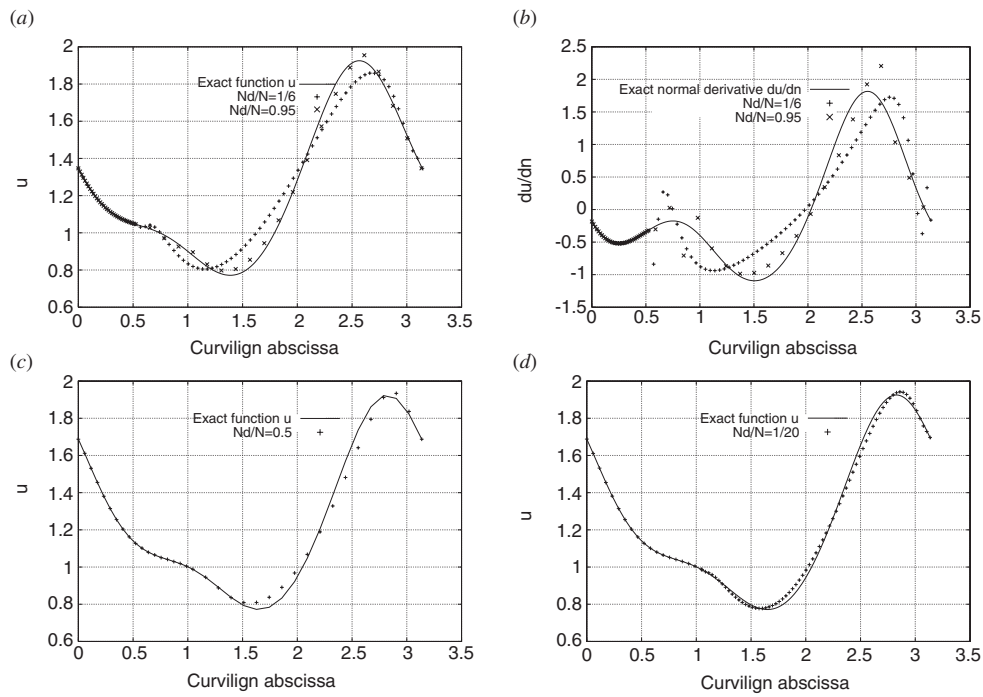


Figure 5. Reconstructions with respect to the ratio of nodes: improvement of the reconstructed data is achieved by redistributing the given number of nodes (a) and (b), whereas no improvement can be achieved by adding nodes on the unknown part (c) and (d).

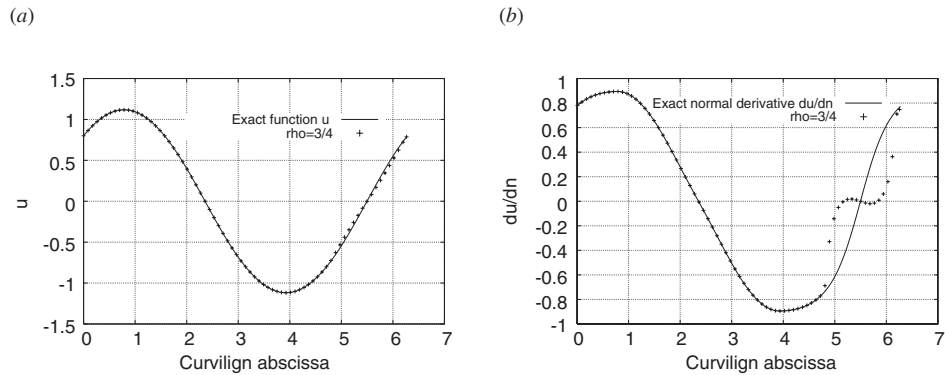


Figure 6. Reconstruction of the function (a) and its normal derivative (b) in the case of singular data resulting from an internal crack.

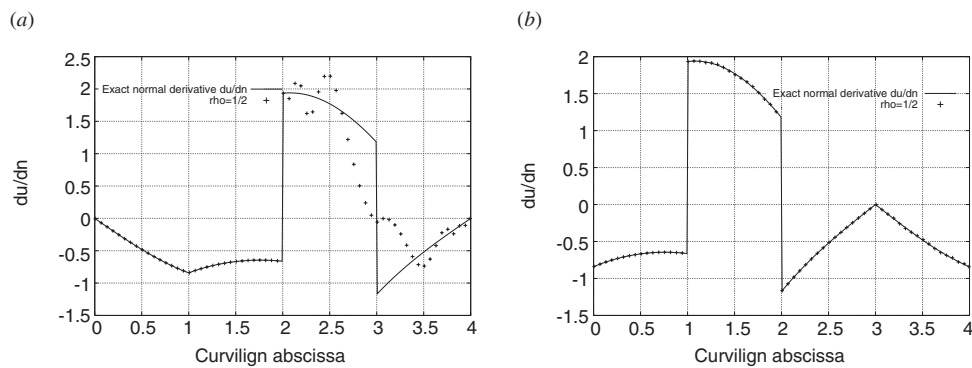


Figure 7. Reconstruction of normal derivatives in the case of non smooth data: square domain with prescribed data on two adjacent (a) or opposite (b) sides.

with large derivatives, whereas in the case that the boundary itself is non-smooth, the normal derivative is discontinuous even if the solution is smooth. Singular solutions may also result from bodies carrying cracks inside. In such a case, the solution is not even harmonic in Ω . In order to retrieve the lacking data, we thus need to consider the problem in a ring-shaped domain lying between Γ and some fictitious boundary surrounding the crack. However, in doing so, we are extending the part of unknown data with respect to that of the prescribed data. Figure 6 displays the reconstructed solution and its normal derivative in such a case, with $\rho = \frac{3}{4}$, which actually means that data are prescribed on $\frac{3}{8}$ of the boundary, including the fictitious part of it. What this example shows is good accuracy in reconstructing the function itself, whereas the reconstruction of its normal derivative is less satisfactory.

Figure 6 shows what may happen in such situations. It is not surprising that the function reconstruction is better than its normal derivative's. As has already been noted, an average approximation of the normal derivative is actually good enough in order to compute with an acceptable accuracy the boundary integrals needed by a reciprocity gap-based algorithm. Besides, the normal derivative is in such a case the given flux, generally prescribed on the whole boundary, which hence needs no reconstruction.

Figures 7(a) and (b) are related to runs on the unit square $[0, 1] \times [0, 1]$, with prescribed data on half the boundary. As for the normal derivative discontinuities, they are well captured

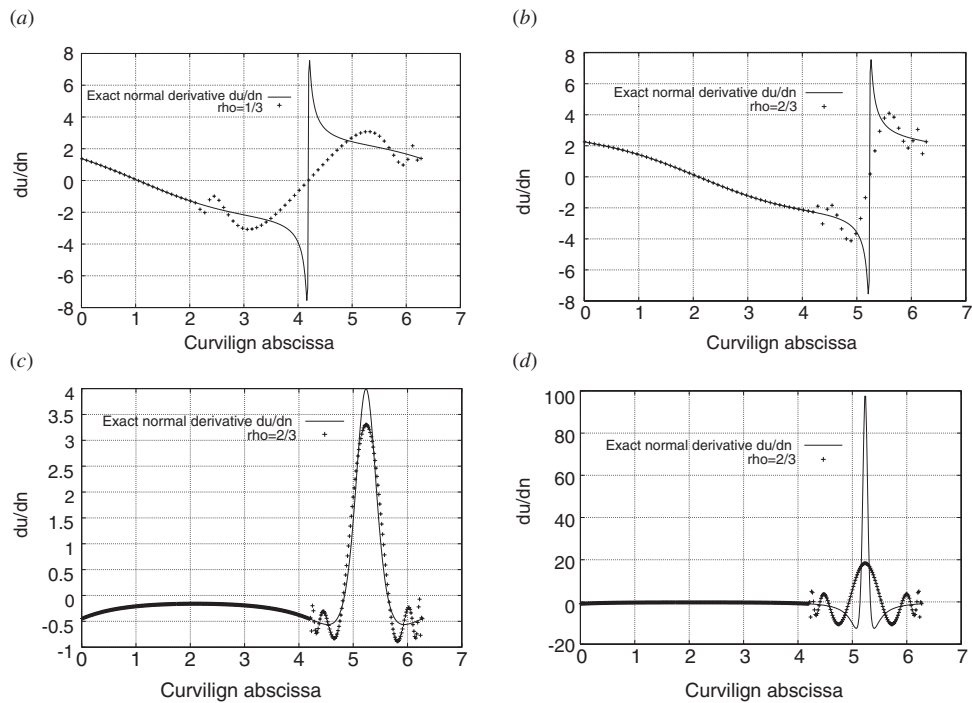


Figure 8. Reconstruction of normal derivatives in the case of non-smooth data: singular function of ‘crack type’ (a), (b); strongly singular functions (c), (d).

in the smart case of prescribed data on two opposite sides of the square, whereas this is no longer the case when the data are prescribed on two successive sides.

Plots (a) and (b) in figure 8 deal with the reconstruction of singular data, coming from the function

$$u_1 := \operatorname{Re} (z - a)^{\frac{1}{2}}$$

where $a = (1.01, 0)$. Plots (c) and (d) display runs with the following ‘singular’ function, with $a = (1.5, 0)$ in the first case and $a = (1.1, 0)$ in the second:

$$u_2 := \operatorname{Re} \frac{1}{(z - a)}.$$

In both cases, the domain is the unit circle. Choosing $a \in \Gamma$, the function u_1 would belong to $H^s(\Gamma)$ for $s < 1$, whereas u_2 would not even belong to $L^2(\Gamma)$. Function u_1 is the singular part of the solution in the case of a cracked domain, a being the crack tip. In both cases, we have been trying to reconstruct the singular part of the data from its smoother part. Although the reconstruction of the function itself causes no problem, the normal derivative ‘discontinuity’ requires, in order to be reasonably captured, that prescribed data be provided on a large enough part of the boundary ($\rho = 2/3$).

4.3.5. Noisy data. We attempt in this section to perform reconstruction from given noisy data, as shown in figure 9. Figure 10 shows the error on the reconstructed function with respect to the noise level on the data. In both cases (noise on u or on $\partial_n u$), the reconstruction is incredibly robust: it resists to a 60% noise level, still reconstructing the data up to a 10%

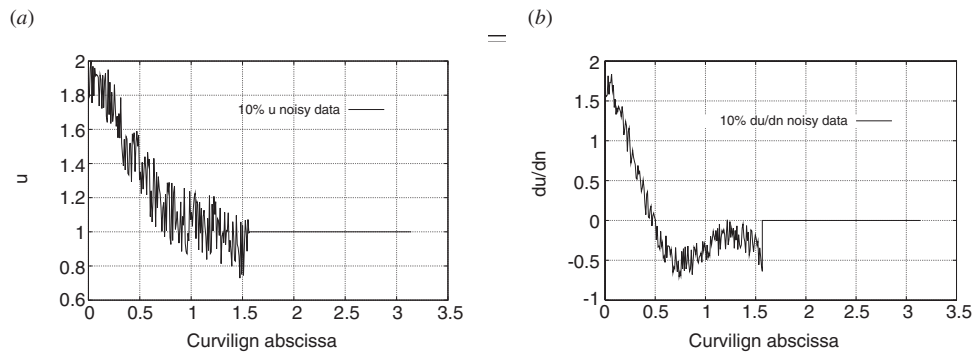


Figure 9. Noisy data: 10% noise on u (a) or on du/dn (b).

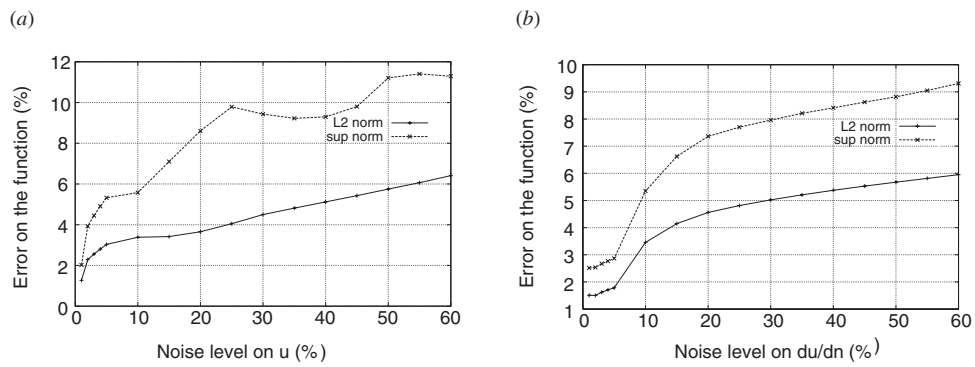


Figure 10. Error on the function reconstruction w.r.t. noise level on u (a) and on du/dn (b).

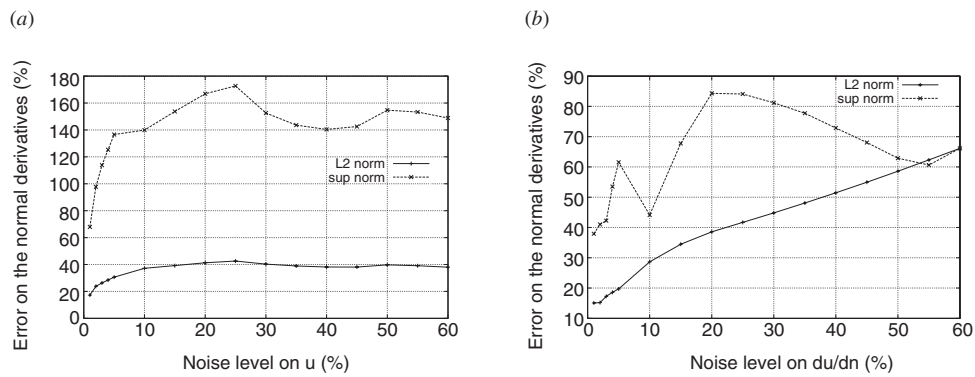


Figure 11. Error on the normal derivative reconstruction w.r.t. noise level on u (a) and on du/dn (b).

maximum norm error or so. As expected, the situation is not so good in regard to the normal derivative reconstruction, as shown by figure 11.

What actually happens is that the algorithm performs a deblurring task on the prescribed Dirichlet data (figure 12(a)), in addition to the reconstruction one, whereas it is not able to get rid in such an efficient way of the noise pollution on the normal derivatives, as pointed out by figure 12(b), the error on the normal derivatives remaining anyway at a somewhat high level.

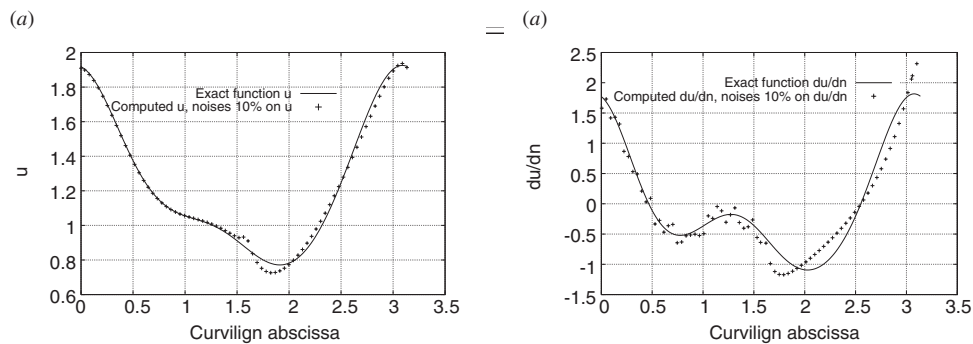


Figure 12. Deblurring 10% noisy Dirichlet (a) or Neumann (b) data.

5. Conclusion

The algorithm we have presented in this paper has several features that make it an effective tool in solving data completion problems:

- *Versatility.* Although the study has been carried out for the Laplacian, there is no obstacle to developing the same approach for other operators, in both 2D and 3D situations. What is needed is simply the ability to solve the forward problem by condensation of the unknowns on the boundary.
- *Accuracy.* The reconstruction is, as expected, better as regards the function itself than its normal derivative. Yet this limitation is not that serious for many purposes, such as crack recovery; developments to come should address this issue, using higher-order versions of the algorithm.
- *Robustness.* The algorithm is resistive to highly noisy data, performing a deblurring task on the given Dirichlet data in addition to the completion one.

The stabilization of the algorithm has been achieved using an iterated Tikhonov regularization method, the additional term in the least square function vanishing while the algorithm converges. It follows that the solution reached does not depend on this term, yet the regularization coefficient impacts the rate of convergence and thus needs to be properly handled.

Several issues remain to be investigated. First, the behaviour of the algorithm in the case of continuous incompatible data needs to be clarified. The main point is to understand what exactly should be meant by ‘noise’, since compatible data are dense in the space of noisy ones. A full numerical analysis of the algorithm, including its rate of convergence with respect to various parameters involved (h , c), in addition to the knowledge of the behaviour of α_h , might help this understanding. Investigating alternative operators, including nonlinear ones, is also a question of great interest. Finally, how far the so-reconstructed data are relevant to applications such as crack recovery is an issue to study from both a numerical and theoretical perspective, in order to confirm the confidence one may reasonably put in the algorithms thanks to the already obtained numerical results.

Acknowledgments

The authors are indebted to both referees for their valuable remarks and comments. The work of MJ is supported by the Tunisian Secretary of State for Research and Technology within the LAB-STI-02 programme.

References

- [1] Adams R A 1975 *Sobolev Spaces* (New York: Academic)
- [2] Andrieux S and Ben Abda A 1996 Identification of planar cracks by complete overdetermined data: inversion formulae *Inverse Problems* **12** 553–63
- [3] Bannour T, Ben Abda A and Jaoua M 1997 A semi-explicit algorithm for the reconstruction of 3D planar cracks *Inverse Problems* **13** 899–917
- [4] Baratchart L and Leblond J 1998 Hardy approximation to L^p functions subsets of the circle with $1 \leq p < \infty$ *Constructive Approximation* **14** 41–56
- [5] Baratchart L, Leblond J, Mandréa F and Saff E B 1999 How can the meromorphic approximation help to solve some inverse problems for the Laplacian? *Inverse Problems* **15** 79–90
- [6] Ben Abda A, Ben Ameer H and Jaoua M 1999 Identification of 2D cracks by elastic boundary measurements *Inverse Problems* **15** 67–77
- [7] Chaabane S and Jaoua M 1999 Identification of Robin coefficients by the means of boundary measurements *Inverse Problems* **15** 1425–38
- [8] Cimetière A, Delvare F and Pons F 2000 Une méthode inverse avec régularisation évanescence *C.R. Acad. Sci., Paris IIb* **328** 639–44
- [9] Engl H 1981 Necessary and sufficient conditions for convergence of regularization methods for solving linear operator equations of the first kind *Numer. Funct. Anal. Optim.* **3** 201–22
- [10] Engl H, Hanke M and Neubauer A 1996 *Regularization of Inverse Problems* (Dordrecht: Kluwer)
- [11] Fasino D and Inglese G 1999 An inverse Robin problem for Laplace's equation: theoretical results and numerical methods *Inverse Problems* **15** 41–8
- [12] Lions J L and Magenes E 1968 *Problèmes Aux Limites non Homogènes et Applications* vol 1 (Paris: Dunod)
- [13] Plato R and Vainikko G 1990 On the regularization of projection methods for solving ill-posed problems *Numer. Math.* **57** 63–79
- [14] Santosa F, Vogelius M and Xu J-M 1998 An effective non linear boundary condition for corroding surface. Identification of the damage based on steady state electric data *Z. Angew. Math. Phys.* **49** 656–79
- [15] Tikhonov A and Arsenine V 1977 *Méthode de Résolution de Problèmes mal Posés* (Moscow: Mir)
- [16] Tikhonov A N, Goncharsky A V, Stepanov V V and Yagola A G 1995 *Numerical Methods for the Solution of Ill Posed Problems* (Dordrecht: Kluwer)